



1 **Wastewater matters: Incorporating wastewater reclamation into a process-based**
2 **hydrological model (CWatM v1.08)**

3

4 Dor Fridman¹, Mikhail Smilovic¹, Peter Burek¹, Sylvia Tramberend¹, Taher Kahil¹
5

6 ¹ Water Security Research Group, Biodiversity and Natural Resources Program, International Institute for Applied
7 Systems Analysis (IIASA), Laxenburg, Austria.
8

9 *Correspondence to:* Dor Fridman (fridman@iiasa.ac.at)

10 **Abstract**

11 Wastewater treatment and reuse are increasingly perceived as essential to improve water use efficiency and
12 increase water availability and reliability. Furthermore, wastewater has a significant impact on hydrological
13 signals in urban watersheds. Hydrological modeling has developed over the last few decades to account for the
14 human-water interface. Yet, despite the importance of wastewater treatment and reclamation, it is not yet
15 comprehensively included in large-scale and multi-resolution hydrological models. This paper presents the newly
16 developed wastewater treatment and reclamation module as part of the hydrological Community Water Model
17 (CWatM) and demonstrates its capabilities and advantages in an urban and watershed with intermittent flows.
18 Incorporating wastewater into the model increases model performance by better-representing discharge during the
19 dry period. It allows for representing wastewater reuse in different sectors and takes on a modular approach,
20 allowing for higher control over the wastewater treatment and reclamation process when spatial resolution and
21 data availability allow it. As the current development focuses on water quantity, the water quality dimension of
22 wastewater treatment remains a limitation, which sets the plans of incorporating water quality into the model and
23 developing global input data for wastewater treatment and reclamation.
24



25

26 **1. Introduction**

27 Hydrological modeling has developed over the last few decades to account for the human-water interface (Wada
28 et al., 2017). Recent developments in this field focused on developing higher-resolution global hydrological
29 models (GHMs) by increasing models' spatial resolution, adjusting their datasets, and including a variety of water
30 management options (Abeshu et al., 2023; Hoch et al., 2023; Burek et al., 2020; Hanasaki et al., 2022).

31 Increasing human interventions in the water cycle and higher spatial resolution modeling have emphasized the
32 need to include water management as an integral part of hydrological models (Hanasaki et al., 2022). Some large-
33 scale hydrological models (LHMs) already account for water management aspects, like water withdrawal and
34 consumption, irrigation management, reservoir operations, water transfers, and desalination (Wada et al., 2017).
35 Wastewater treatment and reclamation are other management options that are increasingly important in many
36 regions. Currently, treated wastewater is estimated at 188 km³ per year globally, which is around 52% of effluents
37 generated. Further, approximately 22% (of treated wastewater) is estimated to be reclaimed (Jones, van Vliet,
38 Qadir, & Bierkens, 2021). Thebo et al. (2017) find that around 35.9 mega hectares of irrigated cropland are
39 supported by rivers dominated by wastewater from upstream urban areas, and Van Vliet et al. (2021) indicate that
40 expansion of treated wastewater uses from 1.6 to 4.0 billion m³ per month can strongly reduce water scarcity
41 levels worldwide.

42

43 Specifically, wastewater reuse is a valuable water source for industrial use and irrigation in water-stressed regions.
44 For example, Israel reclaims around 88% of its treated wastewater, mainly for use in the agricultural sector, where
45 it satisfies about 45% of the agricultural water withdrawals (Fridman, Biran, & Kissinger, 2021). Treated
46 wastewater is also used for irrigation in South European, Mediterranean, and North African countries (Angelakis
47 et al., 1999; Bixio et al., 2006). While accepting exacerbated stress on freshwater resources, the European
48 Parliament is working to improve the quality of wastewater treatment in the EU, aiming to increase wastewater
49 reuse (European Parliament, 2024). It follows that prospects of increased utilization of this resource are plausible.
50 Wastewater collection, treatment, and reclamation are relevant processes for the hydrological modeling of urban
51 catchments and complex water resource systems and are included in different small-scale models (Salvadore,
52 Bronders, & Batelaan, 2015). Large-scale hydrological models often neglect wastewater treatment and
53 reclamation. However, to some extent, few models include wastewater treatment effects on water quality. The
54 Soil & Water Assessment Tool (SWAT) includes septic tanks as an on-site treatment option. It simulates the
55 percolation of wastewater into soils, the interaction between pollutants and the soil media, and bacteria build-up
56 and nutrient uptake (Neitsch, Arnold, Kiniry, & Williams, 2011).

57 Another example is DynQual, a global water quality model coupled with the PCR-GLOBWB2 hydrological model
58 (Jones et al., 2022). The model includes wastewater treatment processes in water quality simulations while
59 simplifying wastewater treatment and reclamation management. Namely, in DynQual, wastewater is generated,
60 collected, treated, and discharged locally (in a single grid cell).

61 While these are significant developments, they only partially capture the complex dynamics between human
62 activities and hydrological processes occurring in urbanized catchments or otherwise complex water resource
63 systems.



64 This paper introduces a recently developed, customizable wastewater treatment and reclamation module as part
65 of the Community Water Model (CWatM), allowing various modes of simulating wastewater treatment and
66 reclamation processes.

67 CWatM is a versatile, fully distributed, modular, and open-source hydrological model that simulates natural and
68 human-affected hydrological processes at a daily time step and multiple spatial resolutions ranging from 0.5° to
69 30 arc-seconds (Burek et al., 2020). CWatM has extensive and publicly available documentation of the source
70 code, the model structure, and model training and tutorials (<https://cwatm.iiasa.ac.at/>, last access: 11 July 2024).

71 The development of the wastewater treatment and reclamation fits with the modularity and flexibility of CWatM
72 by providing various modus-operandi to enable simulation of wastewater treatment and reclamation on global
73 (0.5°), regional (5 arc minutes), and local (up to 30 arc seconds) scales. This paper aims to introduce this module
74 using a hyper-resolution (resolutions of less than or equal to 1 km²) case study of an urbanized river basin in a
75 relatively dry climate (the Ayalon River basin in Israel).

76 The rest of the paper is organized as follows. Section 2 describes the model development; section 3 covers the
77 case study, input data, and scenarios; and section 4 presents the results, followed by discussion and conclusions
78 in sections 5 and 6, respectively.

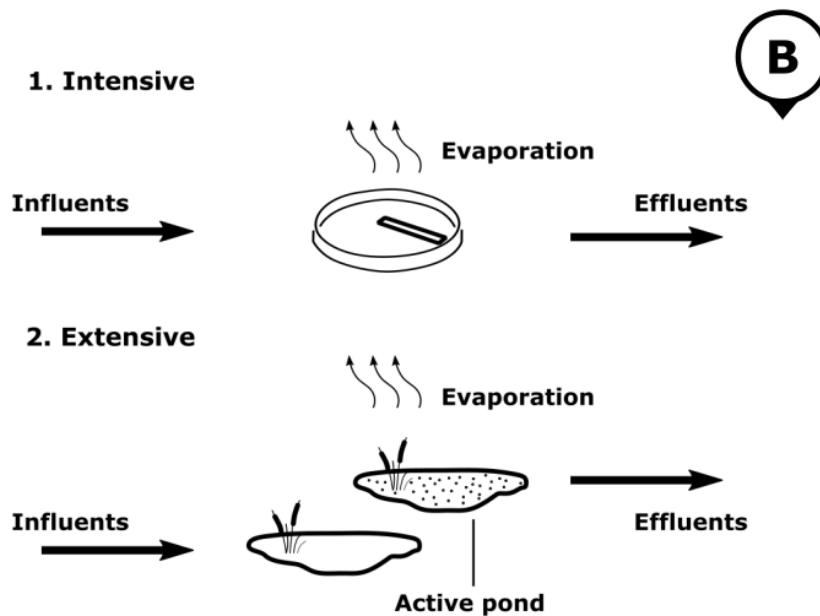
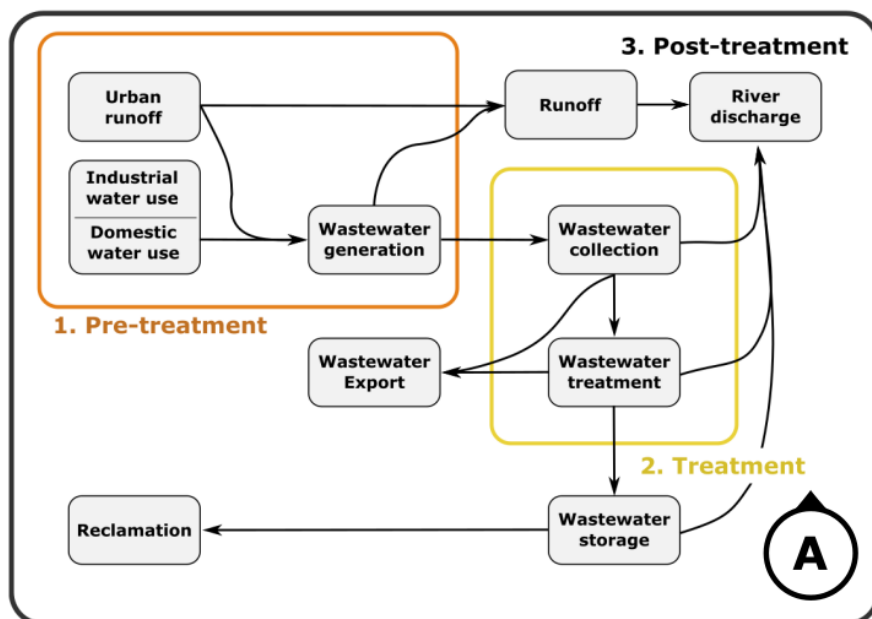
79 **2. Model development**

80 **2.1. The Community Water Model (CWatM)**

81 CWatM is a large-scale distributed hydrological model suitable for implementation at global and regional scales
82 (Burek et al., 2020). It is implemented in the Python programming language and is fully open-source
83 (https://cwatm.iiasa.ac.at). CWatM simulates the main hydrological processes and covers some aspects of the
84 human-water interface. This paper presents the recently developed wastewater treatment module, aiming to
85 enhance CWatM's capacities for addressing human water management. The model is applied to the relatively
86 water-scarce Ayalon River basin in Israel. It uses a spatial resolution of 30 arc-seconds (so-called ~1 km² grid) in
87 a geographic coordinate system (WGS84). Groundwater is simulated by the coupled CWatM-MODFLOW6
88 model (Guillaumot et al., 2022) at a spatial resolution of 500 meters using the UTM36N coordinate system.

89 **2.2. Developing the Wastewater Treatment and Reclamation Module (WRTM)**

90 The wastewater treatment and reclamation module (WRTM) enhances the capacity of CWatM to simulate the
91 human-water interface at hyper-spatial resolution. It introduces wastewater generation, collection, treatment,
92 discharge, storage, and reclamation to CWatM. Figure 1A demonstrates WRTM workflow and sub-modules: (1)
93 pre-treatment; (2) treatment; (3) post-treatment.



94
 95
 96
 97

Figure 1: (A) Workflow of the Wastewater Treatment and Reclamation Module, and (B) the main processes and flows in intensive and extensive wastewater treatment systems.



98

2.2.1. Pre-treatment

99 The first processes of the wastewater module are the accumulation of wastewater and sealed area runoff in each
100 grid cell (see Equation 1). Wastewater originates from domestic and industrial effluents ($Eff_{l,t}^{Dom}$ and $Eff_{l,t}^{Ind}$),
101 calculated by multiplying the simulated non-irrigation return flow as the sectoral fraction of the non-irrigation
102 water demand.

103

104 **Equation 1: Calculating WWTP influents in CwatM-WTRM.**

$$105 \quad Inflow_{j,t} = \sum_{l \in j} (Eff_{l,t}^{Dom} \times D_j^{Dom} + Eff_{l,t}^{Ind} \times D_j^{Ind}) \times Cs_l + Rf_l \times \alpha$$

106 *Note:* j and t represent a simulated WWTP and the time step, respectively; l indicates a grid cell.

107

108 Setting up wastewater treatment plants (WWTP) allows for collecting and treating wastewater from different
109 sectors using a logical variable (e.g., D^{Dom}). The aggregated value of potentially collected effluents is multiplied
110 by a collection share coefficient (Cs) representing sewer connection rates and leakages. Finally, any share of the
111 urban runoff (Rf) can be added to the collected effluents by applying the α collection coefficient. Thus, it is
112 possible to control the design of the urban stormwater drainage systems, either integrated, partially integrated, or
113 completely separated from the urban sewer system.

114

2.2.2. Treatment

115 The treatment phase starts with the collection of influents to WWTP. User-defined collection areas and
116 efficiencies guide this process (see Equation 1). Wastewater treatment plants can hold the following features: the
117 period of operation (e.g., from 2000 to 2010), daily treatment capacity, export share, designed hydraulic retention
118 time (HRT), and minimally allowed HRT. The WWTP inputs use a tabular format (i.e., via an Excel spreadsheet),
119 facilitating the creation of several instances for each WWTP to represent plant upgrades over time (e.g., increased
120 daily capacity, reduction in HRT).

121 Currently, the module supports two optional wastewater treatment technologies defined by the hydraulic retention
122 time. The two options are intensive and extensive treatment plants, as described in Figure 1b. HRT of intensive
123 WWTP usually does not exceed 24 hours, and a treatment plant is considered extensive if its HRT is two days or
124 above, though setting it to 20 -30 days is recommended (Pescod, 1992).

125 The main flows within the treatment section are influent, evaporation, and effluent, as described below.

126 Influent inflows

127 If daily influent exceeds the plant's daily treatment capacity, excess wastewater is discharged into pre-specified
128 discharge locations. Treatment plants' design often allows inflows to exceed the designed capacity to handle
129 fluctuations, for example, due to rain events. The hydraulic retention time is defined as $HRT = Volume/Inflow$,
130 hence exceeding the designed capacity reduces the retention time, resulting in less effective wastewater treatment
131 (Pescod 1992).

132 The module accounts for this feature by enabling treatment plants to have peak capacities higher than their
133 designed capacities. The minimally allowed HRT (days) parameter expresses the lowest operational hydraulic
134 retention time a treatment plant can withstand before it refuses inflows. Following the calculation of the hydraulic



135 retention time, the maximum daily capacity can be calculated as follows $Inflow_{max} = Volume/HRT_{min}$,
136 whereas volume is fixed. For example, a minimally allowed HRT of 0.8 days implies an increase of 25% in the
137 operational daily capacity.

138

139 Evaporation

140 Surface area evaporation is calculated by multiplying the potential open water evaporation rate with the estimated
141 surface area of the treatment pools, and it is limited by the volume of stored wastewater in the pool.

142 Calculating the surface area of the treatment pools is different for intensive and extensive systems. The approach
143 divides daily treatment capacity for intensive systems by an estimated treatment pool depth (currently set to six
144 meters).

145 Extensive systems are modeled as treatment ponds, alternately filling up and treating water (see Figure 1B). Unlike
146 in intensive systems, treatment ponds in extensive systems may remain empty for long periods. Since evaporation
147 is simulated at the pond level, it considers only ponds with positive water storage.

148

149 **Equation 2: calculation of the surface area of extensive treatment systems.**

$$150 \quad A_{S_j} = \frac{1}{Depth_j} \times \left(VolCap_j \times \frac{TreatTime_j}{TreatPool_j - 1} \right)$$

151

152 The surface area of each treatment pool is calculated by dividing the pool's volume by its depth (see Equation 2;
153 *Depth*, currently set to one meter). Each pool volume is derived by multiplying the daily capacity (*VolCap*) with
154 the pool filling time. The latter is a function of the total treatment time (*TreatTime*) and a predefined number of
155 treatment pools (*TreatPool*; currently set to three).

156

157 Effluents

158 Effluents can be discharged, exported, or sent to reservoirs for reclamation. The timing of effluent release differs
159 between intensive and extensive systems. Figure 1B shows the main differences between these two types of
160 systems. Influent remain in the treatment plant during the predefined treatment time in intensive systems. For
161 example, for a treatment time of one timestep, the effluent volume at time t equals the influent volume minus
162 evaporation of time $t - 1$.

163 In an extensive system, we differentiate between two types of treatment ponds. At each time, there is one treatment
164 pond that receives all inflows. All other ponds can be either empty or not. Every pond that is neither a receiving
165 pond nor an empty one is termed an 'active' pond, i.e., where wastewater treatment occurs. Effluents are released
166 from 'active' ponds under any of the following conditions: (a) the predefined treatment time has passed since the
167 'active' pond stopped receiving inflows; (b) all pools are at full capacity, and more inflows should be added into
168 the system. In the latter case, the effluents always originated from the 'active' pond with the longest retention time,
169 though they may not be fully treated.



170

2.2.3. Post-treatment

171 The module has three post-treatment possibilities: river discharge, wastewater export, and reclamation. The
172 module exports untreated and treated wastewater; collected untreated wastewater is exported from the simulated
173 region if the WWTP associated with the collection area does not exist within the model domain. Treated
174 wastewater can be exported to account for cases where reclamation occurs partially or entirely outside the
175 simulated region. In this case, the 'Export share' parameter allows a fixed proportion of the effluents to be sent
176 outside the model domain. In the latter case, the export of treated wastewater occurs immediately after the
177 treatment phase.

178 Reclamation (e.g., for irrigation purposes) generally occurs using the reservoir module, so treated wastewater is
179 sent to reservoirs that manage water use. The module iterates over all treatment plants and attempts to send treated
180 wastewater to associated reservoirs. In the case of multiple reservoirs, the module divides the water in proportion
181 to the reservoirs' remaining storage (calculated as $remainingStorage_{i,t} = totalVolume_i - liveStorage_{i,t}$). If
182 all related reservoirs are full, the module discharges the remaining water in a predefined discharge location.
183 Discharge is the default behavior if no reservoir is associated with a treatment plant. Further, the user can force
184 discharge for specific WWTP, even if reservoirs are associated with them, by setting the export share to -1. Finally,
185 untreated wastewater can be discharged if a plant's inflows exceed the plant's peak capacity (see minimally
186 allowed HRT in section 2.2.2).

187 This module provides multiple wastewater storage, conveyance, and reclamation modeling options. For example,
188 one can simulate the discharge and dilution of treated wastewater into an upstream channel, which can be re-
189 captured in a reservoir downstream for reclamation purposes. Additionally, treated wastewater can be managed
190 in a separate reclamation system by establishing a set of artificial, off-stream (type-4) storage reservoirs. A type-
191 4 reservoir is not connected to the river network, thus having no channel-related inflows or outflows. Instead,
192 water inputs include water/wastewater pumping, and water outputs are evaporation and pumping. As each WWTP
193 can be linked to one or more reservoirs or discharge its water directly into a river channel, the model allows for
194 the combination of the two aforementioned approaches.

195

3. Case study application

196 Israel is located on the Eastern Coast of the Mediterranean between the latitudes 29°N–34°N and along the 35°E
197 longitude. Its Central coastal and Northern parts are governed by a Mediterranean climate (hot and dry summer),
198 its Eastern parts are arid due to rain shadow from its Central Mountain range, and the Southern parts experience
199 a semi- to hyper-arid climate due to their vicinity to the world's desert belt.

200 During the 1960s, Israel initiated a country-wide water conveyance system (the 'National Water Carrier') to
201 transfer water southwards from the northern Sea of Galilee, allowing rural development and large-scale irrigation
202 in the semi-arid Negev region (Tal, 2006). Israel's water system is intensively managed today and relies primarily
203 on seawater desalination, treated wastewater reclamation, and groundwater abstraction. Although it is a nationally
204 managed system, significant regional differences exist in sectoral water provision (Fridman et al., 2021).

205 The Ayalon basin is in central Israel and the West Bank, and stretches 815 km² between the western slopes of the
206 Judea Mountains and the Mediterranean Coastal zone. A few kilometers inland, the Ayalon spills into the Yarkon
207 stream (see Figure 2). Ayalon is an urbanized river basin partially overlaying the Tel Aviv-Yaffo metropolitan



208 area downstream and the city of Modi'in in its middle segment. Downstream urban areas result in considerable
 209 water demand, vast runoff from sealed areas, and a high rate of wastewater generation. Upstream, the landscape
 210 of the Ayalon basin is predominantly a rural mosaic of open areas and small settlements. Patches of irrigated
 211 agriculture and forests are primarily found in the South-Eastern parts of the basin.

212 Ayalon is a seasonal river originating in the South-Eastern part of the basin. An artificial 'horseshoe' shaped
 213 reservoir ('Mishmar Ayalon') regulates its flows and maintains relatively fast groundwater recharge. Five main
 214 tributaries drain the remaining basin and feed the Ayalon River downstream. An artificial cemented canal collects
 215 the river water before crossing densely populated urban areas downstream.

216 3.1. Data sources

217 This hyper-resolution analysis combines global and local datasets better to represent the case-study hydrologic
 218 processes and human-hydrologic interactions (Hanasaki et al., 2022). Table 1 provides an overview of both the
 219 global (e.g., meteorological forcings, soil characteristics, topography, and the river network) and the local datasets
 220 (e.g., wastewater treatment and reclamation, reservoir networks, aquifer properties, landcover maps, seawater
 221 desalination, and water demand).

222

223 **Table 1: Model inputs from global and local datasets.**

Input data	Spatial resolution	Data sources
Global datasets		
Meteorological forcings	0.5° grid; daily Downscaling to 30 arc-seconds	ISIMIP 3a, GSWP3-W5E5 (Lange, Mengel, Treu, & Büchner, 2022) WorldClim (Fick & Hijmans, 2017)
Soil	30 arc-seconds	Dai et al. (2019) Shangguan, Hengl, Jesus, Yuan, & Dai (2017)
Topography	3 arc-seconds	MERIT Digital Elevation Model (Yamazaki et al., 2017)
River network properties flow direction map	30 arc-seconds	MERIT Hydro IHU (Eilander et al., 2020)
Local/modified datasets		
Landcover maps	500 meters	MODIS Global landcover between 2001 - 2019 (Friedl & Sulla-Menashe, 2019), OpenStreetMap (Urba areas, water, and green spaces; available at https://www.openstreetmap.org), Ministry of Agriculture and Rural Development (MOAG, 2022; cultivated land), and Hamaarag (2017; forests' map)



Municipal and industrial water demand	Municipality	Israel Central Bureau of Statistics (ICBS, 2022). A Random Forest regression imputed missing data for different localities and specific years. Palestinian Central Bureau of Statistics (PCBS, 2022).
Wastewater treatment plants' location and treatment levels, collection areas, and wastewater generation coefficients	Municipality	A national dataset was compiled mainly relying on a report by the Israel National Reserve Authority (INRA, 2016) and data from PCBS (2022a).
Desalination	National	Annual desalination capacity between 2005 - 2019 (Gov.il, N.D.). A basin-scale desalination is allocated proportionally to the relative domestic water demand. For example, the national supply of desalinated seawater in 2005 and 2015 was 20 and 503.4 MCM, respectively. In the same years, the Ayalon desalinated seawater supply is estimated at 3.4 and 88 MCM.
Reservoirs	-	Manually identify and digitize reservoirs based on aerial photography and satellite imagery. Depth and volume were assumed based on fieldwork and engagement with water managers.
Groundwater basin and aquifers	Various resolutions	Aquifer maps were taken from Israel Hydrological Services (2014), and porosity and permeability were taken from Melloul et al. (2006) for the coastal basin and from Wollmann, Calvo, & Burg (2009) for the mountain basin.

224

225 Groundwater basins and aquifers

226 This case study uses the coupled CWatM-Modflow model to account for the interface between surface and
 227 groundwater hydrology and groundwater dynamics (Guillaumot et al., 2022). The Ayalon River basin lies above
 228 two principal groundwater aquifers. The west mountain aquifer is part of the larger Yarkon-Tanimin aquifer
 229 system and has two partially separated sub-aquifers reaching a thickness of 600 meters. It comprises carbonate
 230 sedimentary rocks and has a relatively high but non-homogenous hydraulic conductivity (Wollmann, Calvo, &
 231 Burg, 2009). The slopes of the West Judea mountains function as recharge zones, and the top layers in the Western



232 foothills are made of chalk and marl and act as an aquitard, confining the Western Mountain aquifer (see Figure
233 A1). To the west, the relatively shallow Coastal aquifer (thickness up to 200 meters) mixes a sandstone aquifer
234 with clay lens, resulting in varying hydraulic conductivity (Melloul, Albert, & Collin, 2006). Data on groundwater
235 abstraction volumes and locations, as well as the water table changes, was unavailable.

236

237 Reservoirs

238 We have manually identified and digitized reservoirs in the Ayalon basin using multiple data sources, including
239 georeferenced aerial photography, visual inspection of satellite imagery, fieldwork, and interviews with local
240 water management experts. The biggest reservoir in the Ayalon basin is Mishmar Ayalon (7.5 MCM; Figure 2),
241 a seasonal water storage fed by the upstream section of the Ayalon River and regulates downstream flows. The
242 Natuf reservoir is located on a prior quarry site northeast of the basin (4.3 MCM) and contributes to groundwater
243 recharge. Four smaller reservoirs constitute the wastewater irrigation infrastructure and have a total designed
244 storage of 634,200 m³. This reclamation system extends beyond the basin's borders, for which we account by
245 exporting a fraction of the treated wastewater.

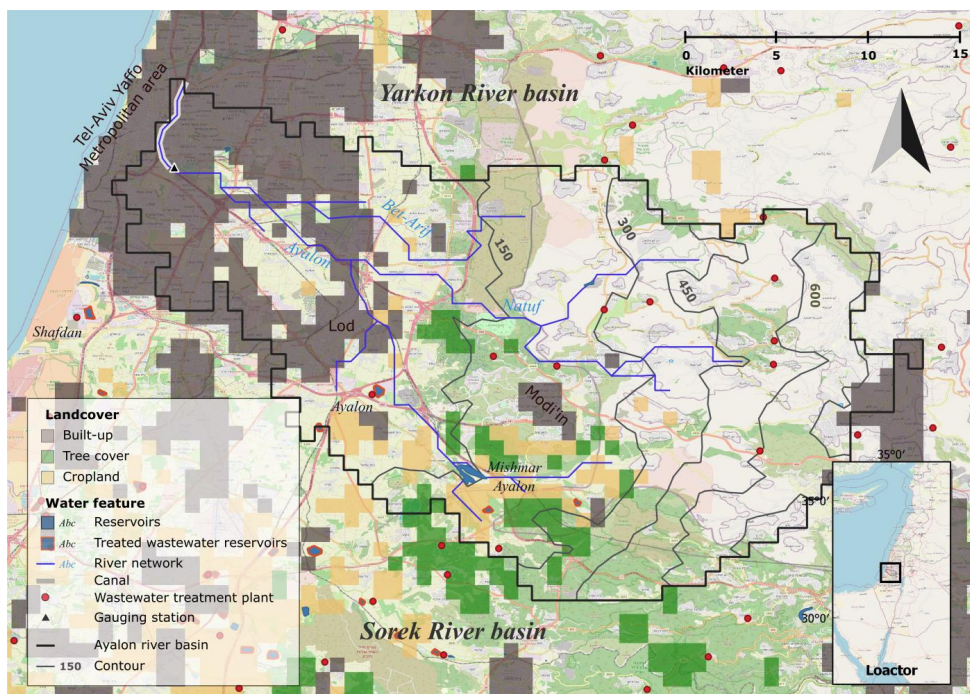
246

247 Wastewater in the Ayalon basin

248 Two primary wastewater treatment plants collect wastewater generated in the main cities, and small-scale
249 treatment plants collect those generated in the rural sector. The *Shafdan* WWTP treats all wastewater generated
250 in the Tel Aviv-Jaffa metropolitan area in the adjacent Sorek basin, which is out of the scope of this analysis.
251 Later, they were exported to the North-Western Negev for irrigation purposes (Fridman et al., 2021). The Ayalon
252 WWTP is the most significant facility in the basin, with a daily capacity of 81,000 m³. It collects treated
253 wastewater from the cities of Lod and Modi'in (see Figure 2) and their surroundings. An extensive treatment plant
254 has been in place since 1995, but development and population growth have exceeded its capacity, increasing sewer
255 discharge frequency into the stream. An intensive activated sludge treatment plant with a daily capacity of 54,000
256 m³ started operating in 2003. Its capacity was increased in 2019. Almost ten small-scale wastewater treatment
257 plants in the Ayalon basin are treating sewers at a settlement scale with a total daily capacity of 12,298 m³.

258

259



260

261 **Figure 2: the Ayalon River basin case study: land cover and major water features. Partially uses data from ©**
 262 **OpenStreetMap contributors 2022. Distributed under the Open Data Commons Open Database License (ODbL) v1.0.**

263

3.2. Setting modeling scenarios and model parameters

264

In this analysis, we simulate the Ayalon basin hydrology and wastewater treatment and reclamation under different scenarios, aiming to explore the effects of the wastewater treatment module's different modes of operation on model calibration and basin-scale water resource management. Table 2 describes the four scenarios. We use scenario S2 for model calibration, which resulted in an urban runoff collection share of 46% of the urban runoff. We explore two different reclamation schemes, using a buffer of four grid cells around the reservoirs (S2) or predefined reclamation zones (S3).

269

Table 2: Description of scenarios and features

Scenario	Wastewater treatment	Urban runoff collection share	Wastewater reclamation
S0: No wastewater	Off	0%	-
S1: No urban runoff collection	On	0%	Irrigation around reclamation reservoirs
S2: With urban runoff collection	On	46%	Irrigation around reclamation reservoirs
S3: Extended pre-irrigation	On	46%	Irrigation in pre-determined reclamation areas

271



272 Additional parameters used for calibration are associated with evapotranspiration rates of irrigated croplands and
273 grassland, soil depth adjustment, within grid-cell soil moisture spatial distribution, soil hydraulic conductivity and
274 water content at saturation, Manning's roughness coefficient, riverbed exchange rate, urban evaporation
275 coefficient, and urban infiltration coefficient. The emphasis on the urban landscape is due to the relatively high
276 share of built-up areas in the Ayalon basin (see Figure 2).

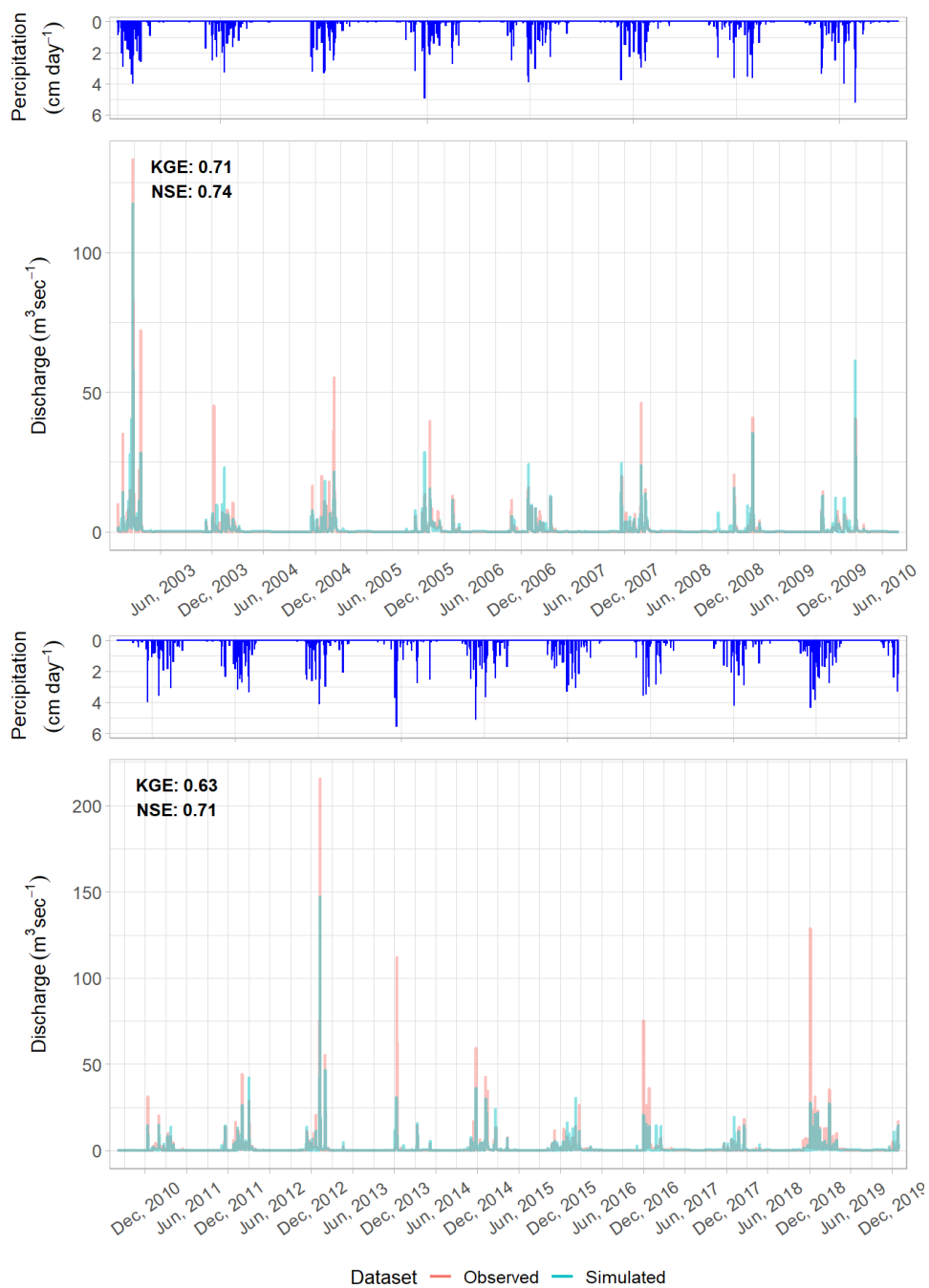
277 **4. Results**

278 **4.1. Model validation**

279 We have calibrated the Ayalon case study against the daily average discharge at the Ayalon-Ezra gauging station
280 (34.794° E, 32.04° N; Figure 2) over the period January 1st, 2003, to July 30th, 2010, and validated over the period
281 August 1st, 2010 to December 31st, 2019. We have also compared the simulated evapotranspiration with a satellite-
282 derived product (Mu, Maosheng, Running, & Numerical Terradynamic Simulation Group, 2014) and the
283 simulated monthly influent flows into the Ayalon WWTP with observed data between 2016 -2019 (Ayalon Cities
284 Association, 2021).

285 The simulation reproduces daily discharge in the Ayalon basin with a KGE of 0.69 and NSE of 0.74. Both
286 validation periods perform relatively well, showing a slight decrease in performance in the latest period ($KGE_{2010-2014} = 0.67$, $KGE_{2015-2019} = 0.5$). The mean observed and simulated discharge at the outlet are 0.81 and 0.89 m³ s⁻¹
287 (see Table 3), respectively. The average simulated discharge is slightly higher than the observations, but the
288 opposite occurs during high-flow days (Figure 3).

290 Regarding evapotranspiration, both the observed and simulated data show clear seasonal patterns, where
291 evapotranspiration is high during the summer, demonstrating overall steady interannual levels (see Figure B1).
292 The model overestimates the evapotranspiration during the late spring and early summer (April – June),
293 presumably due to the under-representation of plant mortality in unmanaged open areas (represented as grassland
294 in the model). Nevertheless, during mid-summer, simulated evapotranspiration is higher than the observations.
295 Evaluating for model performance results in a relatively low KGE (0.33) and NSE (0.35).



296
297
298

Figure 3: comparison of the observed and simulated discharge at the outlet during the calibration and validation periods.



299 Modeling the intermittent Ayalon River case study is challenging, mainly due to its arid climate and small basin
 300 area. Under these conditions, even a low deviation in the absolute simulated discharge results in a high relative
 301 error. It follows that diverting return flows (i.e., sewers) away from the river was a crucial step in the Ayalon
 302 model calibration. Introducing wastewater treatment and reclamation into CWatM enables the simulation of actual
 303 water dynamics in the Ayalon basin, resulting in a better-performing model. The KGE values of scenarios S0-S3
 304 are -1.13, 0.25, 0.61, and 0.62, and the percentage differences between the simulated and observed average
 305 discharge are 201%, 60%, 9.8%, and 7.5%, respectively (see Table 3). The improvement from including the
 306 wastewater treatment and reclamation module (scenario S1) is associated with reducing the dry season's baseflow
 307 from an average of $1.21 \text{ m}^3 \text{ s}^{-1}$ to $0.15 \text{ m}^3 \text{ s}^{-1}$. The effects of urban runoff collection were mainly evident in the
 308 wet season's discharge, which was reduced from an average of $2.46 \text{ m}^3 \text{ s}^{-1}$ (scenario S1) to $1.67 \text{ m}^3 \text{ s}^{-1}$ (scenario
 309 S2). The collection of urban runoff into the sewer systems reduces flows downstream to urban areas and allows
 310 for the capture, to some extent, of the inflow dynamics into the Ayalon wastewater treatment plant (see Figure 5).
 311 Finally, the extended irrigation in scenario S3 results in reduced discharge of treated wastewater into the river
 312 channel and improved model performance.

313 **Table 3: Model performance under different scenarios**

Scenario	KGE	NSE	Annual mean discharge (% relative to observed)	Dry season's mean discharge (% relative to observed)	Wet season's mean discharge (% relative to observed)
Observed	-	-	0.81 ± 4.9 (-)	0.04 ± 0.38 (-)	1.59 ± 6.9 (-)
S0: No wastewater	-1.13	0.59	2.44 ± 5.2 (201%)	1.21 ± 0.61 (2900%)	3.68 ± 7.1 (131%)
S1: No urban runoff collection	0.25	0.64	1.3 ± 5.06 (60%)	0.15 ± 0.56 (275%)	2.46 ± 6.9 (55%)
S2: With urban runoff collection	0.61	0.7	0.89 ± 3.87 (9.8%)	0.12 ± 0.36 (200%)	1.67 ± 5.35 (5%)
S3: Extended irrigation	0.62	0.7	0.87 ± 3.87 (7.4%)	0.1 ± 0.35 (150%)	1.65 ± 5.35 (3.7%)

314

315 4.2. Component and flows of the wastewater module

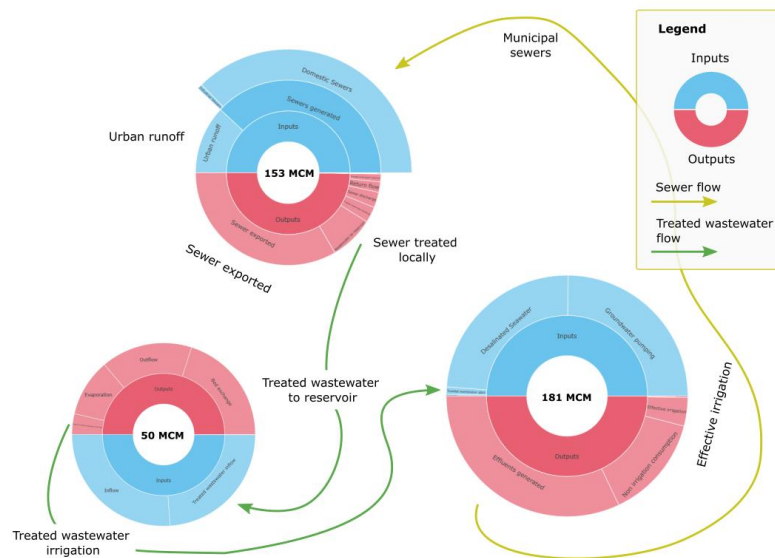
316 The wastewater flows between the different model components are illustrated in Figure 4 using the water circle
 317 concept (Smilovic et al., 2024). Wastewater treatment plants' inflows consist of domestic or industrial wastewater
 318 and are optionally combined with urban runoff (e.g., in dual-purpose urban drainage systems). In the Ayalon basin
 319 case study, the largest share (66%) of the influents is being treated in the *Shafdan* WWTP outside of the basin of
 320 interest (i.e., Sewer exported; see also Figure 2), and approximately 16% are sent to reclamation reservoirs from
 321 local treatment plants. The remaining share includes the discharge of treated wastewater (6%) and sewer overflow
 322 (6%).



323 In Israel, treated wastewater is operated separately from potable water, and reclamation reservoirs do not receive
324 stream inflows; instead, they only store treated wastewater. Roughly half the reservoirs' inflows in the Ayalon
325 basin are of treated wastewater. A large share of the total inflows is lost to evaporation, and approximately 6% is
326 reclaimed for irrigation.

327 According to the second scenario (S2), the Ayalon basin water supply heavily relies on groundwater abstraction
328 (50%) and desalinated seawater (48%). In comparison, wastewater reclamation only plays a minor role
329 (approximately 2% of the water use). Nevertheless, treated wastewater satisfies about 26% of the basin's effective
330 irrigation. Wastewater reclamation in other basins also relies on sewers generated in the Ayalon basin, as all the
331 sewers of the Tel-Aviv metropolitan areas are treated in the *Shafdan* WWTP and used for irrigation in the South
332 of Israel (Fridman et al., 2021).

333



334

335 **Figure 4: Average annual sewer and treated wastewater flows within and between CWatM modules, based on a**
336 **simulation for the Ayalon River Basin, Israel, from 1/1/2001 -31/12/2010.**

337

4.3. Modelling wastewater and urban stormwater collection systems

338 CWatM supports two main hydrological processes of urban areas, namely surface runoff and return flows (e.g.,
339 sewer discharge). Managing these flows utilized either separated or combined collection and drainage systems. In
340 Israel, two separate systems operate to collect urban wastewater and stormwater. However, stormwater leakage
341 into the sewers frequently occurs due to illegal connections of urban drainage to the sewers.

342 The runoff collection coefficient allows the user to control the magnitude of systems integration. One combined
343 system would have a coefficient of one, implying all urban runoff flows into the sewers collection system, and a
344 coefficient of zero suggests two completely separated systems. The calibrated model ended up with a coefficient
345 of 0.46, implying that 46% of urban runoff flows into the sewers.

346 Although the runoff collection coefficient significantly increased model performance, it may lead to slightly
347 overestimating the discharge. Validating the model against wastewater collection data for the Ayalon WWTP also



348 supports the notion that the runoff collection coefficient should have been lower. On average, between 2016 and
349 2019, the Ayalon WWTP accepted 1,780 +/- 85 thousand m³ sewers every month. The average inflows in the
350 scenarios without and with urban runoff collection are 1,562 +/- 119 and 1,682 +/- 195 thousand m³ per month,
351 respectively. Overall, the model underestimates the inflow to the Ayalon WWTP, as shown in the top panel of
352 Figure 5, during the dry months (e.g., April to June). The monthly variation of inflows is partially captured (bottom
353 panel of Figure 5), yet irregularities are missed (e.g., May to August 2017) since water demand inputs into the
354 model are annual.
355 Rain events during the wet season often result in increased inflows into the wastewater treatment plants (e.g.,
356 during December 2016 or January 2018). This increase is only visible in scenarios that include urban runoff
357 collection. The calibrated model overestimates peak flows (see Figure 5 bottom panel), implying that a lower
358 urban runoff collection coefficient is required.



359
360 **Figure 5: Observed VS. simulated monthly wastewater inflows into the Ayalon WWTP with and without urban runoff**
361 **collection using absolute values (top chart) and annually detrended values (bottom chart).**

362 4.4. Modelling wastewater reclamation

363 Wastewater treatment and reclamation may significantly affect water management, particularly for complex water
364 resource systems in water-scarce countries. Israel is a water-scarce country that reclaims wastewater, utilizes
365 desalination water, and transfers water between river basins to mitigate water stress. As Israel manages water
366 nationally, analyzing water resources on a basin scale aligns differently from Israel's actual state of water
367 resources. Instead, the following scenarios aim to illustrate the relevance of the WRTM module to water resource
368 management, as it can be applied to one or multiple basins.



369 Table 4 summarizes the annual average key water sources and uses across the four scenarios. On average, the
 370 annual total natural and alternative water use in the Ayalon basin is estimated at 89 million cubic meters (MCM),
 371 of which almost 7.5% is used for irrigation (6.6 MCM).

372 **Table 4: Key indicators of water use and supply for all four scenarios (annual average in the Ayalon basin between**
 373 **1/1/2001 to 31/12/2019)**

Variable	S0	S1	S2	S3
Irrigation consumption (MCM)	6.6	6.6	6.6	6.6
Treated wastewater irrigation (MCM)	0	1.7	1.8	3.7
Treated wastewater irrigation (exported; MCM)	0	39	51.1	51.1
Groundwater pumping (MCM)	49.4	48.6	48.6	46.7
Sea desalination (MCM)	38.9	38.9	38.9	38.9
Total natural and alternative water (MCM)	88.3	89.3	89.3	89.3
Share treated wastewater irrigation (%)	0%	26%	27%	56%
Share treated wastewater of total natural and alternative water (%)	0%	2%	2%	4%

374 Note: Total natural and alternative water includes groundwater pumping, sea desalination, and treated wastewater irrigation.
 375 Wastewater used outside the basin is excluded.

376
 377 The water supply in the Ayalon basin heavily relies on desalination and groundwater pumping, accounting for
 378 96% -98% of the total water use across all scenarios. Considering only irrigation water, wastewater reclamation
 379 satisfies 26% to 56% of the basin scale withdrawal for irrigation, depending on scenarios. Introducing wastewater
 380 reclamation into CWatM was initially based on irrigation buffer; irrigation with reclaimed wastewater is allowed
 381 within a fixed distance from the reservoirs. In the 'extended irrigation' scenario (S3), the reservoirs are linked with
 382 designated command areas, which reduces the overlap between irrigation areas and increases the irrigation water
 383 withdrawn from each reservoir. Under this scenario, wastewater reclamation accounts for 56% of the total
 384 irrigation and 4% of the total water withdrawal. Reclaimed wastewater as an alternative source for crop irrigation
 385 reduces the pressure on the groundwater resources by 1.6% – 5.5%, as groundwater pumping reduces from 49.9
 386 MCM to 46.7 MCM in scenario S3, relative to the baseline scenario. In practice, the total volume of wastewater
 387 reclamation is much higher since approximately 51 MCM of wastewater is collected in the Ayalon basin, treated
 388 in the nearby *Shafdan* WWTP (in a nearby basin), and reclaimed for irrigation approximately 80 kilometers
 389 southwards.



390

5. Discussion

391 **Wastewater treatment and reclamation play a crucial role in the hydrological modeling of urban**
392 **watersheds, especially in low-discharge/intermittent rivers.**

393 Discharges from wastewater treatment plants often dominate urban watersheds' hydrological signals, increasing
394 low-flows, flashiness, and the frequency of medium and high-flow events (Coxon et al., 2024). The effect of
395 wastewater on stream hydrological signals would become more pronounced in intermittent streams, challenging
396 model calibration. Acknowledging this fact, one may compromise on model performance in urban watersheds,
397 yet including wastewater treatment and reclamation in the modeling allows for increased model performance as
398 it better represents local water management processes. The example provided in this paper demonstrates this point
399 by showing a significant increase in model performance due to including wastewater treatment and reclamation
400 in the modeling.

401 To our knowledge, only a few existing hydrological models account for wastewater treatment and reclamation.
402 Dyn-Qual, for example, simplifies the treatment process and only allows for indirect reclamation, i.e., treated
403 water is discharged into rivers and can be abstracted downstream. SWAT model represents wastewater treatment
404 by including pit latrines, yet both models focus on the water quality and missing critical operations associated
405 with water quantity (e.g., supplying treated wastewater directly to reservoirs or fields). Although addressing the
406 highly relevant topic of water quality, the representation of wastewater processes in these two models would not
407 contribute to model calibration in urban or intermittent watersheds.

408 The importance of including wastewater treatment and reclamation in hyper-resolution (i.e., ~1km) hydrological
409 modeling is also aligned with recent findings, as these models are susceptible to the effects of human activity on
410 the water cycle and often require better representation of these processes and more precise data (Hanasaki et al.,
411 2022). The Ayalon case study relies on local knowledge and data to better represent the in-situ water process and
412 human intervention in the water cycle, which is further emphasized by the inclusion of local knowledge about the
413 leakage of urban stormwater into the sewer collection system (scenario S2), and more accurate data covering the
414 actual command-areas utilizing treated wastewater (scenario S3).

415

416 **The wastewater treatment module is designed to foster synergies across multiple model features to better**
417 **represent the human dimension of the water cycle.**

418 The community water model (CWatM) development is an ongoing effort to provide open-source and readily
419 available modeling tools for basin-scale and large-scale hydrological simulation, and it focuses on the complex
420 and diverse set of interactions between human and water systems. The WRTM development relied significantly
421 on currently available and developing model features. It follows that the case study described in this paper uses
422 three additional water management options and can potentially utilize others. CWatM's source-sector abstraction
423 fraction and reservoir operation options play a pivotal role in modeling the treated wastewater reclamation. The
424 scope of the WTRM includes wastewater generation, collection, treatment, and discharge into a channel or
425 reservoir. Reclamation occurs as a part of the model's water demand routine when channel water is pumped
426 downstream to the treatment plant discharge point or treated wastewater from a reservoir is used to satisfy water
427 demand in their surroundings.

428 Defining reservoirs' command areas that represent, for example, the irrigation areas served by each modeled
429 reservoir allows higher control over the simulated reclamation. As a result, the model can better utilize the existing



430 treated wastewater stock by avoiding overlaps between command areas. Using the source-sector abstraction
431 fraction option also enables significant control over potential water use by defining the potential water mix of
432 different sectors (e.g., irrigation or industrial). For example, defining the irrigation abstraction fraction of treated
433 wastewater to 100% enables water demand to be fully satisfied by treated wastewater in case a sufficient volume
434 of water is available. The treated wastewater in the Ayalon case study is used for crop irrigation, urban landscape
435 irrigation, and thermal power plant cooling. As data on water demand for urban landscape irrigation and thermal
436 power plant cooling was unavailable, this paper only accounts for reclamation by irrigation.

437 While relying mainly on existing model processes, representing the water supply networks in the Ayalon case
438 study required additional development. Water distribution in Israel is pursued via two separate distribution
439 networks for freshwater and reclaimed water. To account for this, an off-stream-network reservoir was introduced
440 to CWatM (also called a type-4 reservoir). The inflows into this reservoir consist only of water transfers, and the
441 outflows are limited to abstraction and evaporation losses. The water levels in these reservoirs are not affected
442 directly by river flows and runoff, and they can maintain a traceable stock of treated wastewater over the long run.

443

444 **The flexibility in the module design is a key concept for developing versatile LHM, that is fit for both**
445 **continental and global simulations and hyper-resolution local simulations. It also allows for the adjustment**
446 **of modeling practices to data availability.**

447 The Community Water Model, as well as other large-scale hydrological models (Hanasaki et al., 2022; Hoch et
448 al., 2023), is shifting towards a multi-resolution modeling framework, allowing users to work on a global scale
449 with coarser resolutions and on a local scale with higher resolutions. As shown in this paper (as well as in Hanasaki
450 et al., 2022), higher (or hyper-) resolution hydrological modeling requires better data and representation of the
451 crucial process in the area of interest as the representation of this process may still be necessary at larger scales
452 (e.g., continental, global), such data may not be fully available. To address this issue, the development of the
453 WRTM adopted a modular approach, allowing modeling with minimal data requirements at higher scales and
454 coarser resolutions but providing additional features to improve the simulation, which can be triggered if data
455 exists. This is demonstrated by the already significant improvement in model performance due to simply including
456 wastewater treatment and reclamation (scenario S1), whereas additional, but relatively smaller, improvements are
457 associated with the inclusion of local knowledge used for triggering optional model features. The use of local
458 knowledge and data is not restricted only to urban stormwater leakage or better representing the irrigation
459 command areas but also to represent the increased capacity and change of treatment technology in the main
460 WWTP (Ayalon) in the river basin. At the current development stage, the optional features include the possibility
461 to restrict wastewater influents into specific plants (e.g., setting separated treatment plants for industrial sewers),
462 export a fixed share of the treated wastewater, allowing leakage from the urban stormwater management system
463 to the wastewater collection system, and provide increased operational capacity to handle peak flows (e.g., with
464 the minimum HRT parameter).

465

466 6. Conclusions

467 The recent progress of large-scale hydrological models toward hyper-resolution requires a better representation
468 of local processes and data. The representation of wastewater treatment and reclamation remains a gap across



469 most models, and it has significant implications for model performance in intermittent rivers and urban
470 watersheds.

471 This paper introduces a novel wastewater treatment and reclamation model development within a large-scale
472 multi-resolution hydrological model. It demonstrates its added value in terms of enhanced model performance
473 and the inclusion of essential processes, such as wastewater reclamation. Further, it introduces a recommended
474 development framework that relies on a diverse set of existing features and aims to achieve high flexibility, so it
475 is less restricted by data availability and can be easily customized to different spatial resolutions.

476 As wastewater is naturally associated with water quality, this aspect remains a limitation within the scope of the
477 current development and will be addressed in future developments. The module can benefit from forming a global
478 dataset and additional wastewater treatment technologies.

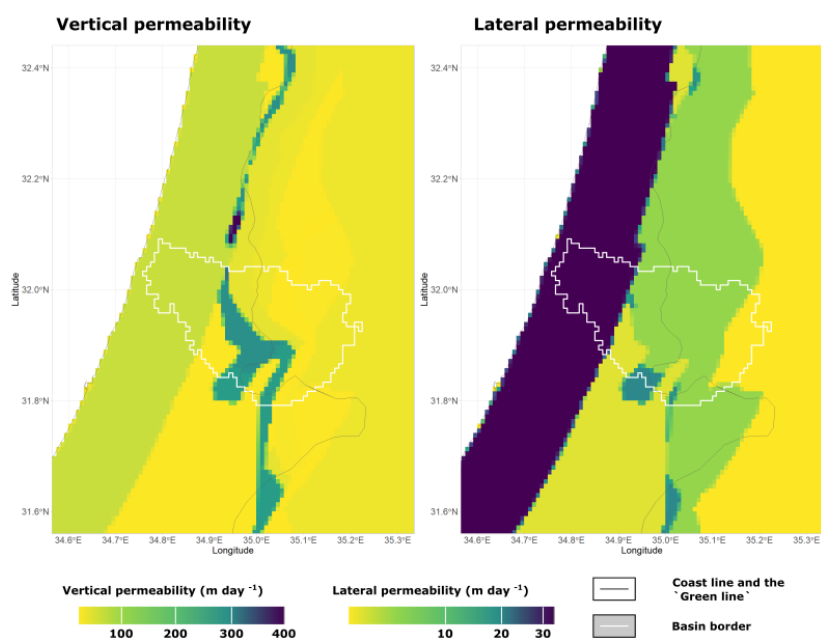
479



480 **7. Appendices**

481 Appendix A

482 Figure A1 describes the vertical and lateral permeability of the YARTAN and coastal aquifers in Israel. The
483 coastal aquifer forms a relatively narrow stripe stretching North to the South. Next, the western mountain aquifer
484 is located towards the east, showing a relatively diverse permeability. The YARTAN groundwater basin includes
485 the western mountain aquifer but extends far beyond the borders of the Ayalon River basin.
486



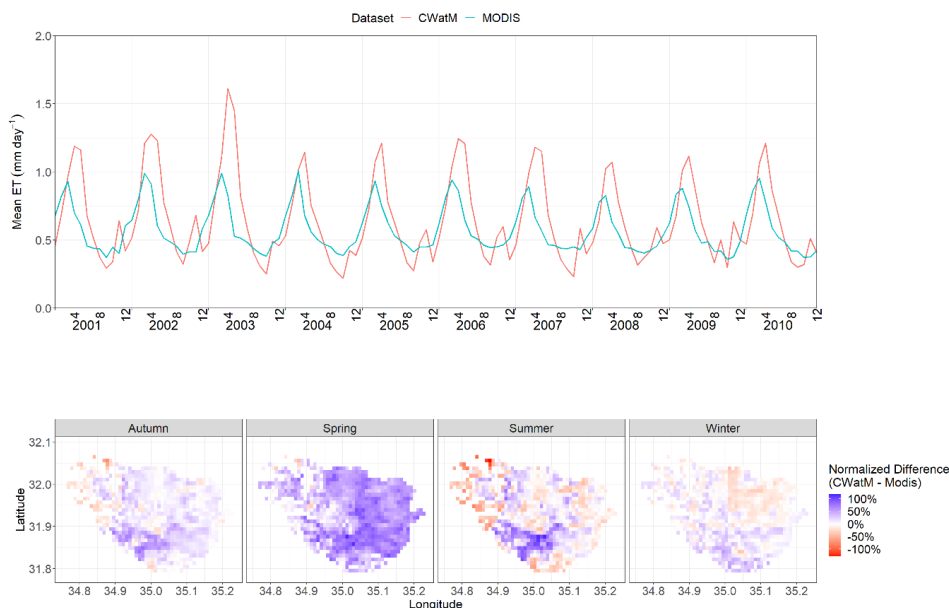
487

488 **Figure A1: Vertical and lateral permeability in the YARTAN and Coastal aquifers in the Ayalon basin and its**
489 **surroundings.**

490

491 Appendix B

492 Figure B1 compares the simulated evapotranspiration with observed data derived from the MODIS sensor.



493

494 **Figure B1: Comparing observed and simulated monthly terrestrial evapotranspiration (top) and seasonal gridded**
495 **normalized difference for 2005.**

496

497

498 8. Code and Data Availability

499 CwatM source code is publicly available on GitHub under the following repository:

500 <https://github.com/iiasa/CWatM>; the most recent version is currently available under the development branch and
501 will be included in the next public release.

502 The data used for this case study is available at: <https://zenodo.org/doi/10.5281/zenodo.12752966>, and the model
503 used for running the simulations had some additional modifications for the Israel case study and can be found at:

504 <https://github.com/dof1985/CWatM-Israel>.

505 9. Author contributions

506

507 DF, MS, and PB developed the module code (Wastewater treatment and reclamation), and prepared model input
508 and observation datasets. DF, MS, and PB have prepared model inputs. DF performed the simulations and
509 associated post-processing, and prepared the paper with contributions from MS, PB, ST, and TK. MS, ST, and
510 TK acquired the funding and were in charge of project administration and supervision.



511 **10. Competing interests**

512 The contact author has declared that none of the authors has any competing interests.

513 **11. Disclaimer**

514 Any opinions, findings, and conclusions or recommendations expressed in this material do not necessarily reflect
515 the views of the funding organizations..

516 **12. Financial support**

517 This research has received support from the SOS-Water project (Grant Agreement: 101059264) funded under the
518 European Union's Horizon Europe Research and Innovation Programme and the GATWIP project funded by the
519 Innovation and Bridging Grants Fund of IIASA. The work of Dor Fridman was partially funded by the IIASA-
520 Israel Post-Doctoral program.

521 **13. References**

- 522 Abeshu, G. W., Tian, F., Wild, T., Zhao, M., Turner, S., Chowdhury, A. F. M. K., Vernon, C. R., Hu, H., Zhuang,
523 Y., Hejazi, M., and Li H.: Enhancing the representation of water management in global hydrological models.
524 *Geoscientific Model Development*, 16(18), 5449–5472. <https://doi.org/10.5194/gmd-16-5449-2023>, 2023.
- 525 Angelakis, A., Marecos Do Monter, M. H. F., Bontoux, L., and Asano, T.: The status of wastewater reuse practice
526 in the Mediterranean basin: need for guidelines. *Water Res.*, 33(10): 2201-2217. [https://doi.org/10.1016/S0043-1354\(98\)00465-5](https://doi.org/10.1016/S0043-1354(98)00465-5), 1999.
- 527
528 Ayalon Cities Association.: Wastewater treatment plant Ayalon-Nesher - Annual report for 2020.
529 <https://ayalonn.co.il/%d7%93%d7%99%d7%95%d7%95%d7%97%d7%99%d7%9d-%d7%a9%d7%a0%d7%aa%d7%99%d7%99%d7%9d/>, last access: 2/8/2022, 2021
- 530
531 Bixio, D., Thoeye, C., de Koning, J., Joksimovic, D., Savic, D., Wintgens, T., and Melin, T.: Wastewater reuse in
532 Europe. *Desalination*, 187(1): 89-101. <https://doi.org/10.1016/j.desal.2005.04.070>, 2006.
- 533 Burek, P., Satoh, Y., Kahil, T., Tang, T., Greve, P., Smilovic, M., Guillaumot, L., Zhao, F., and Wada, Y.:
534 Development of the Community Water Model (CWatM v1.04) – a high-resolution hydrological model for global
535 and regional assessment of integrated water resources management. *Geoscientific Model Development*, 13(7),
536 3267–3298. <https://doi.org/10.5194/gmd-13-3267-2020>, 2020.
- 537 Coxon, G., McMillan, H., Bloomfield, J. P., Bolotin, L., Dean, J. F., Kelleher, C., Slater, L., and Zheng, Y.:
538 Wastewater discharges and urban land cover dominate urban hydrology across England and Wales, EGU General
539 Assembly 2024, 14-19 Apr 2024, EGU24-5850, <https://doi.org/10.5194/egusphere-egu24-5850>, 2024.
- 540 Dai, Y., Xin, Q., Wei, N., Zhang, Y., Shanguan, W., Yuan, H., Zhang, S., Liu, S., and Lu, X.: A Global High-
541 Resolution Data Set of Soil Hydraulic and Thermal Properties for Land Surface Modeling. *Journal of Advances
542 in Modeling Earth Systems*, 11(9), 2996–3023. <https://doi.org/10.1029/2019MS001784>, 2019.
- 543 European Parliament.: New EU rules to improve urban wastewater treatment and reuse (News: press releases,
544 published 10-04-2024). [https://www.europarl.europa.eu/news/en/press-room/20240408IPR20307/new-eu-rules-
545 to-improve-urban-wastewater-treatment-and-](https://www.europarl.europa.eu/news/en/press-room/20240408IPR20307/new-eu-rules-to-improve-urban-wastewater-treatment-and-)



- 1546 [reuse#:~:text=EU%20countries%20will%20be%20required.especially%20in%20water%2Dstressed%20areas,](#)
1547 last access: 10/7/2024, 2024.
- 1548 Eilander, D., Winsemius, H. C., Van Verseveld, W., Yamazaki, D., Weerts, A., and Ward, P. J.: MERIT Hydro
1549 IHU [Dataset]. <https://doi.org/10.5281/zenodo.5166932>, 2020.
- 1550 Fick, S. E., and Hijmans, R. J.: WorldClim 2: new 1-km spatial resolution climate surfaces for global land areas.
1551 *International Journal of Climatology*, 37(12), 4302–4315. <https://doi.org/10.1002/joc.5086>, 2017.
- 1552 Fridman, D., Biran, N., & Kissinger, M.: Beyond blue: An extended framework of blue water footprint accounting.
1553 *Science of The Total Environment*, 777, 146010. <https://doi.org/10.1016/j.scitotenv.2021.146010>, 2021.
- 1554 Friedl, M. and Sulla-Menashe, D.: MCD12Q1 MODIS/Terra+Aqua land cover type yearly L3 Global 500m SIN
1555 Grid V006 NASA EOSDIS Land Processes DAAC [Dataset], 2019.
- 1556 Guillaumot, L., Smilovic, M., Burek, P., Bruijn, J. de, Greve, P., Kahil, T., and Wada, Y.: Coupling a large-scale
1557 hydrological model (CWatM) with a high-resolution groundwater flow model to assess the impact of irrigation at
1558 regional scale. *Geoscientific Model Development Discussions*, 2022, 1–37. [https://doi.org/10.5194/gmd-2022-](https://doi.org/10.5194/gmd-2022-161)
1559 [161](#), 2022.
- 1560 Israeli Government portal.: Desalination volumes by year. [https://www.gov.il/BlobFolder/reports/desalination-](https://www.gov.il/BlobFolder/reports/desalination-structures/he/%D7%9E%D7%AA%D7%A7%D7%A0%D7%99%20%D7%94%D7%AA%D7%A4%D7%9C%D7%94%20%D7%91%D7%99%D7%A9%D7%A8%D7%90%D7%9C.pdf)
1561 [structures/he/%D7%9E%D7%AA%D7%A7%D7%A0%D7%99%20%D7%94%D7%AA%D7%A4%D7%9C%](#)
1562 [D7%94%20%D7%91%D7%99%D7%A9%D7%A8%D7%90%D7%9C.pdf](#), last accessed: 1/4/2022, 2022.
- 1563 Hamaarag.: Vegetation map of Israel's natural and forested areas, 2017. <https://hamaarag.org.il>, last accessed: 1-
1564 4-2022, 2017.
- 1565 Hanasaki, N., Matsuda, H., Fujiwara, M., Hirabayashi, Y., Seto, S., Kanae, S., and Oki, T.: Toward hyper-
1566 resolution global hydrological models including human activities: application to Kyushu island, Japan. *Hydrology*
1567 *and Earth System Sciences*, 26(8), 1953–1975. <https://doi.org/10.5194/hess-26-1953-2022>, 2022.
- 1568 Hoch, M. J., Sutanudjaja, E. H., Wanders, N., van Beek, R. L. P. H., and Bierkens, M. F. P.: Hyper-resolution
1569 PCR-GLOBWB: opportunities and challenges from refining model spatial resolution to 1 km over the European
1570 continent. *Hydrol. Earth Syst. Sci.*, 27: 1383-1401. <https://doi.org/10.5194/hess-27-1383-2023>, 2023.
- 1571 ICBS.: Municipal data in Israel 1999-2021 [Dataset].
1572 [https://www.cbs.gov.il/he/publications/Pages/2019/%D7%94%D7%A8%D7%A9%D7%95%D7%99%D7%95](https://www.cbs.gov.il/he/publications/Pages/2019/%D7%94%D7%A8%D7%A9%D7%95%D7%99%D7%95%D7%AA-%D7%94%D7%9E%D7%A7%D7%95%D7%9E%D7%99%D7%95%D7%AA-%D7%91%D7%99%D7%A9%D7%A8%D7%90%D7%9C-%D7%A7%D7%95%D7%91%D7%A6%D7%99-%D7%A0%D7%AA%D7%95%D7%A0%D7%99%D7%9D-%D7%9C%D7%A2%D7%99%D7%91%D7%95%D7%93-1999-2017.aspx)
1573 [%D7%AA-%D7%94%D7%9E%D7%A7%D7%95%D7%9E%D7%99%D7%95%D7%AA-](#)
1574 [%D7%91%D7%99%D7%A9%D7%A8%D7%90%D7%9C-%D7%A7%D7%95%D7%91%D7%A6%D7%99-](#)
1575 [%D7%A0%D7%AA%D7%95%D7%A0%D7%99%D7%9D-](#)
1576 [%D7%9C%D7%A2%D7%99%D7%91%D7%95%D7%93-1999-2017.aspx](#), last accessed: 14/2022, 2022.
- 1577 INRA.: Wastewater collection, treatment, and recalculation for irrigation purposes – a national survey 2014.
1578 [https://www.google.com/url?sa=t&rct=j&q=&esrc=s&source=web&cd=&cad=rja&uact=8&ved=2ahUKEwimn](https://www.google.com/url?sa=t&rct=j&q=&esrc=s&source=web&cd=&cad=rja&uact=8&ved=2ahUKEwimn9aF7Z6GAXRBdsEHTj0DEwQFnoECBIQAQ&url=https%3A%2F%2Fwww.gov.il%2FBlobFolder%2Freports%2Ftreated_waste_water1%2Fhe%2Fwater-sources-status_kolhin_kolhim_2014.pdf&usq=AOvVaw3RjSAodJvw9NF0XD9h6qWY&opi=89978449)
1579 [9aF7Z6GAXRBdsEHTj0DEwQFnoECBIQAQ&url=https%3A%2F%2Fwww.gov.il%2FBlobFolder%2Frepor](#)
1580 [ts%2Ftreated_waste_water1%2Fhe%2Fwater-sources-](#)
1581 [status_kolhin_kolhim_2014.pdf&usq=AOvVaw3RjSAodJvw9NF0XD9h6qWY&opi=89978449](#), last accessed:
1582 1/4/2022, 2016.
- 1583 Israel Hydrological Services.: Hydrologic data - Annual report - The state of the water resources 2014.
1584 <https://www.gov.il/he/departments/publications/reports/water-resources-2014>, last accessed: 1/4/2022, 2014.



- 585 Jones, E. R., Bierkens, M. F. P., Wanders, N., Sutanudjaja, E. H., van Beek, L. P. H., and van Vliet, M. T. H.:
586 DynQual v1.0: A high-resolution global surface water quality model. *Geoscientific Model Development*
587 *Discussions*, 2022, 1–24. <https://doi.org/10.5194/gmd-2022-222>, 2022.
- 588 Jones, E. R., Vliet, M. T. H. van, Qadir, M., and Bierkens, M. F. P.: Country-level and gridded estimates of
589 wastewater production, collection, treatment and reuse. *Earth System Science Data*, 13(2), 237–254.
590 <https://doi.org/10.5194/essd-13-237-2021>, 2021.
- 591 Lange, S., Mengel, M., Treu, S., and Büchner, M.: ISIMIP3a atmospheric climate input data. ISIMIP Repository
592 [Dataset]. <https://doi.org/10.48364/ISIMIP.982724>, 2022.
- 593 Melloul, A., Albert, J., and Collin, M.: Lithological Mapping of the Unsaturated Zone of a Porous Media Aquifer
594 to Delineate Hydrogeological Characteristic Areas: Application to Israel's Coastal aquifer. *African Journal of*
595 *Agricultural Research*, 1(3), 47–56, 2006.
- 596 Ministry of Agriculture and Rural Development of Israel (MOAG): Cultivated lands map, online GIS resource
597 [Dataset]. [https://data1-
598 moag.opendata.arcgis.com/datasets/f2cbce5354024da28f93788c53b182d2_0/explore?location=31.747323%2C3
599 4.905146%2C12.88](https://data1-moag.opendata.arcgis.com/datasets/f2cbce5354024da28f93788c53b182d2_0/explore?location=31.747323%2C34.905146%2C12.88), last accessed: 1/4/2022, 2022.
- 600 Mu, Q., Maosheng, Z. Running, S. W., and Numerical Terradynamic Simulation Group.: MODIS Global
601 terrestrial evapotranspiration (ET) product MOD16A2 collection 5 [Dataset], 2014.
- 602 Neitsch, S. L., Arnold, J. G., Kiniry, J. R., and Williams, J. R.: Soil and water assessment tool - Theoretical
603 documentation - Version 2009. Texas Water Resources Institute, 2011.
- 604 OpenStreetMap contributors. (2022). Planet dump retrieved from <https://planet.osm.org>.
605 PCBS.: Water statistics in Palestinian territory 2001-2008 [Dataset].
606 https://www.pcbs.gov.ps/PCBS_2012/Publications.aspx?CatId=33&scatId=312, last accessed: 1/4/2022, 2022.
- 607 PCBS.: Wastewater statistics in Palestina territory.
608 https://www.pcbs.gov.ps/PCBS_2012/Publications.aspx?CatId=33&scatId=312, last accessed: 1/4/2022, 2022a.
- 609 Pescod, M. B.: Wastewater treatment and use in agriculture - FAO irrigation and drainage paper 47, 1992.
- 610 Salvatore, E., Bronders, J., and Batelaan, O.: Hydrological modelling of urbanized catchments: A review and
611 future directions. *Journal of Hydrology*, 529, 62–81. <https://doi.org/10.1016/j.jhydrol.2015.06.028>, 2015.
- 612 Shangguan, W., Hengl, T., Jesus, J. Mendes de, Yuan, H., and Dai, Y. Mapping the global depth to bedrock for
613 land surface modeling. *Journal of Advances in Modeling Earth Systems*, 9(1), 65–88.
614 <https://doi.org/10.1002/2016MS000686>, 2017.
- 615 Smilovic, M., Burek, P., Fridman D., Guillaumot, L., de Bruijn, J., Greve, P., Wada, Y., Tang, T., Kronfuss, M.,
616 and Hanus, S.: Water circles-a tool to assess and communicate the water cycle. *Environ. Res. Lett.*, 19: 021003.
617 <https://doi.org/10.1088/1748-9326/ad18de>, 2024.
- 618 Tal, A.: Seeking Sustainability: Israel's Evolving Water Management Strategy. *Science*, 313(5790), 1081–1084.
619 <https://doi.org/10.1126/science.1126011>, 2006.
- 620 Thebo, A. L., Drechsel, P., Lambin E. F., and Nelson, K. L.: A global, spatially-explicit assessment of irrigated
621 croplands influenced by urban wastewater flows. *Env. Res. Lett.*, 12(7): 074008, [https://doi.org/10.1088/1748-
622 9326/aa75d1](https://doi.org/10.1088/1748-9326/aa75d1), 2017.



623 Van Vliet, M. T. H., Jones, E. R., Flörke, M., Franssen, W. H. P., Hanasaki, N., Wada, Y., and Yearsley, J. R. :
624 Global water scarcity including surface water quality and expansions of clean water technologies. *Env. Res. Lett.*,
625 16: 024020. <https://doi.org/10.1088/1748-9326/abbfc3>, 2021.

626 Wada, Y., Bierkens, M. F. P., Roo, A. de, Dirmeyer, P. A., Famiglietti, J. S., Hanasaki, N., Konar, M., Liu, J.,
627 Müller Schmied, H., Oki, T., Pokhrel, Y., Sivapalan, M., Troy, T. J., van Dijk, A. I. J. M., van Emmerik, T., van
628 Huijgevoort, M. H. J., van Lanen, H. A. J., Vörösmarty, C. J., Wanders, N., and Wheeler, H.: Human–water
629 interface in hydrological modelling: current status and future directions. *Hydrology and Earth System Sciences*,
630 21(8), 4169–4193. <https://doi.org/10.5194/hess-21-4169-2017>, 2017

631 Wollmann, S., Calvo, R., and Burg, A. A three-dimensional two-layers model to explore the hydrologic
632 consequences of uncontrolled groundwater abstraction at Yarkon-Taninim Aquifer - Final report.
633 <https://www.gov.il/he/departments/publications/reports/wollman-et-al-report-2009>, last accessed: 1/4/2022, 2009.

634 Yamazaki, D., Ikeshima, D., Tawatari, R., Yamaguchi, T., O'Loughlin, F., Neal, J. C., Sampson, C. C., Kanae, S.,
635 and Bates, P. D. A high accuracy map of global terrain elevations. *Geophysical Research Letters*, 44, 5844–5853.
636 <https://doi.org/10.1002/2017GL072874>, 2017.

637

638